

Title: Utilizing Radiolabeled 3'-deoxy-3'-[¹⁸F]fluorothymidine with Positron Emission Tomography to Monitor the Effect of Dexamethasone on Non-Small Cell Lung Cancer.

Authors: Christopher I. McHugh¹, Monica R. Thipparthi¹, Jawana M. Lawhorn-Crews^{1,2}, Lisa Polin^{1,2}, Shirish Gadgeel³, Janice Akoury^{1,2}, Thomas J. Mangner¹, Kirk A. Douglas^{1,2}, Jing Li^{1,2}, Manohar Ratnam^{1,2}, and Anthony F. Shields^{1,2*}

Affiliations:

¹Wayne State University School of Medicine, Detroit, MI.

²Karmanos Cancer Institute, Detroit, MI.

³Department of Oncology, University of Michigan Health System, Ann Arbor, MI.

***Address for correspondence:** Anthony F. Shields, M.D., Ph.D., 4100 John R., HW04HO, Detroit, MI 48201. Phone: (313) 576-8735. E-mail: shieldsa@karmanos.org.

First Author: Christopher I. McHugh, 540 E Canfield St, Detroit MI 48201. Phone: (734) 277-6612. E-mail: cmchugh@med.wayne.edu. Author is a graduate student.

Disclaimer: None of the materials presented herein have been published or are under consideration elsewhere. The authors declare no conflicts of interest.

Word Count: 4994

Financial Support: This work was partially funded by the NIH Grant P30 CA22453 and Department of Defense contract W81XWH-11-1-0068.

ABSTRACT

Non-small cell lung cancer (NSCLC) is a leading cause of cancer mortality in the United States and pemetrexed-based therapies are regularly used to treat non-squamous NSCLC. Despite widespread use, pemetrexed has a modest effect on progression-free survival, with varying efficacy between individuals. Recent work has indicated that dexamethasone, given to prevent pemetrexed toxicity, is able to protect a subset of NSCLC cells from pemetrexed cytotoxicity by temporarily suppressing of the S-phase of the cell cycle. Therefore, dexamethasone may block treatment efficacy in a subpopulation of patients, and could be contributing to the variable response to pemetrexed.

Methods: Differences in retention of the experimental positron emission tomography (PET) tracer 3'-deoxy-3'-fluorothymidine (FLT) were used to monitor S-phase suppression by dexamethasone in NSCLC cell models, animals with tumor xenografts, and patients with advanced cancer. **Results:** Significant reductions in tracer uptake were observed after 24h dexamethasone treatment in NSCLC cell lines and xenograft models expressing high levels of glucocorticoid receptor alpha, coincident with pemetrexed resistance visualized by attenuation of the 'flare' effect associated with pemetrexed activity. 2/4 patients imaged in a pilot study with ^{18}F -FLT-PET following dexamethasone treatment demonstrated reductions in tracer uptake from baseline, with variable response between individual tumor lesions. **Conclusions:** ^{18}F -FLT-PET presents a useful method for the non-invasive monitoring of dexamethasone-mediated S-phase suppression in NSCLC and could provide a method for the individualization of chemotherapy in patients receiving pemetrexed-based regimens.

Keywords: Imaging, PET, Lung cancer, Dexamethasone, FLT

INTRODUCTION

Lung cancer is the leading cause of cancer-related mortality in the United States, accounting for 27% of cancer deaths (1). Non-small cell lung cancer (NSCLC) comprises 83% of lung cancers, and the majority of patients have advanced disease at the time of diagnosis (1). Several randomized clinical trials have shown that pemetrexed, given as a monotherapy or in combination with a platinum-containing compound, is a preferred chemotherapeutic for the treatment of advanced non-squamous NSCLC (2-4). Pemetrexed is a folate anti-metabolite that causes cytotoxicity primarily through inhibition of thymidylate synthase (TS) (5,6). Although widely used, pemetrexed has a modest but variable effect in patients, with a median increase in progression-free survival of 5.3 months in the front-line setting when combined with cisplatin, and only 3.3 months when used as monotherapy (4,7). Furthermore, the 5-year survival for metastatic NSCLC remains dismal, at less than 4% (8). Given this paradigm, it is critical to identify factors that can be used to predict and optimize the clinical benefit of pemetrexed in order to maximize efficacy and spare non-responders the toxicity of ineffective chemotherapy. Several studies have observed an association between low tumor expression of TS and better outcomes in patients treated with pemetrexed (9). However, this has not been shown to be a powerful independent predictor of patient response to pemetrexed, and is not used clinically (10).

Despite its relatively mild toxicity profile, a major adverse effect of pemetrexed is the manifestation of a generalized, painful, pruritic skin rash (11). To protect against this rash, patients are routinely administered 4 mg of dexamethasone twice daily starting the day before therapy and continuing until the day after treatment (12). In addition, dexamethasone is frequently used as an anti-emetic for patients receiving cisplatin or carboplatin (13). Dexamethasone is a synthetic glucocorticoid that upon binding to glucocorticoid receptor alpha (GR α) modulates genes involved in cell proliferation and apoptosis, as well as inflammation and the inflammatory response (14,15). Recently, dexamethasone, in a GR α -dependent fashion, has been found to cause reversible G1 cell cycle arrest in NSCLC cells, resulting in the protection of cells from pemetrexed cytotoxicity (16). Since the biological half-life of dexamethasone is substantially longer than that of pemetrexed (36-54

and 2.5 hours respectively), this may represent a significant clinical problem. Histologic examination of NSCLC lesions has suggested there is an approximately equal distribution of tumors with high and low GR α expression (17). It is possible the protective effect of dexamethasone, combined with differential tumor GR α expression may explain, in part, the variable efficacy of pemetrexed in clinical practice. It is therefore desirable to develop a technique that can be used to ascertain the GR α level and potential pemetrexed resistance in patients. Analysis of biopsy specimens is likely inadequate for this task given the enormous clonal heterogeneity observed within solid tumors and between metastatic foci (18,19). This is especially relevant in this case, as NSCLC patients receiving pemetrexed typically have advanced disease.

A rapid and non-invasive technique to functionally image the effect of dexamethasone on NSCLC over a patient's entire cancer burden would be to monitor retention of 3'-deoxy-3'-fluorothymidine (FLT), developed for use with positron emission tomography (PET). Radiolabeled FLT is taken up by tumor cells and trapped intracellularly via phosphorylation by the S-phase-specific enzyme thymidine kinase 1 (TK1) (20). Changes in FLT retention can therefore be used to monitor the effect of compounds such as dexamethasone, which alter cell cycle progression (21). Uptake of FLT is reproducible and has been shown to correlate with the proliferation marker Ki-67 in NSCLC (22-24). Here FLT retention was applied as a direct functional probe to measure dexamethasone-mediated S-phase suppression in NSCLC. Additionally, the study sought to use ¹⁸F-FLT accumulation to monitor the effect of pemetrexed *in vivo*. The basis for this was the observation that compounds that inhibit *de novo* thymidine biosynthesis, such as pemetrexed, elicit a transient increase in FLT uptake due to up-regulation of thymidine salvage, termed the 'flare' phenomenon (25,26). This effect was recently shown in cell lines as well as mice bearing NSCLC tumors and may provide a way to visualize the interference of dexamethasone with pemetrexed activity *in vivo* (27).

MATERIALS AND METHODS

³H-FLT Uptake Measurements

All cell lines were authenticated using the Promega PowerPlex® 16 System. Technical details concerning tissue culture and generation of recombinant H1299-GR α cells are described elsewhere (13). NSCLC cells were seeded 5×10^5 cells/well in 6-well plates with glucocorticoid-depleted media. Cells were incubated in 100 nM dexamethasone, corresponding to the peak plasma concentration in humans after a single oral dose (28). Cells treated with pemetrexed were incubated with 5 μ M for 4h. After treatment, cells were transferred to media containing approximately 1600 Bq 3 H-FLT and incubated for 1 hour. Cells were washed, lysed with 1M KOH, and mixed with 5 mL of Ultima Gold XR scintillation cocktail. Sample activity was measured by a liquid scintillation analyzer (Packard Tricarb) and normalized to cell number using a parallel experiment and cell counting via the trypan blue exclusion method. All experiments were performed in triplicates.

Establishment of NSCLC Xenografts and Animal Imaging Protocol

Subcutaneous xenografts were established by implanting cubic fragments (~2 by 2 by 2 mm) of tumor tissue bilaterally into the axilla of 4-6 week old female SCID/NCr mice (Charles River), and animals were placed on study when tumors reached an average volume of 250 mm³. Mice were treated intraperitoneal (ip) with veterinary grade dexamethasone (15 mg/kg twice daily), which allowed for steady-state serum concentrations within the pharmacological effective range (28,29) (Supplemental Table 1). Animals treated with pemetrexed were administered 10 mg/kg intravenously, and were fed a low-folate diet starting 10 days prior to treatment. Animals were injected intravenously (iv) with approximately 9.5 MBq of 18 F-FLT, synthesized as published (30). One hour following tracer injection, mice underwent a 10-minute emission scan using a MicroPET scanner (Concorde Microsystems R4). 6-8 mice were used for each treatment condition. Animals were each imaged at baseline and following the specified treatments; each animal served as its own control when comparing change before and after treatment. Reconstructed images were evaluated with PMOD and tracer activity within tumors was corrected for decay and converted to standardized uptake values (SUVs). Data is expressed in terms of SUV_{max}, which reflects the activity of the hottest pixel within the tumor.

Patient Imaging

To determine if dexamethasone-mediated effects on FLT retention could be observed in a clinical setting, a small pilot study was conducted in patients at the Karmanos Cancer Institute. Patients were considered eligible for the study if they were diagnosed with non-squamous NSCLC, were scheduled to receive a chemotherapy regimen that included dexamethasone, had no history of prior pemetrexed or docetaxel chemotherapy, had measurable disease with at least one lesion ≥ 2 cm on CT/MR, and could tolerate two PET scans. We planned to image five patients were consented to join the study, only four of the consented patients completed the evaluation. Patients were injected with ^{18}F -FLT (range: 167-265 MBq; mean: 226 MBq) over 60 seconds and images were collected 1 hour later using a PET/CT scanner (GE Discovery STE). Patients were imaged at baseline and again 24h after the start of oral dexamethasone treatment (4 mg twice daily) as is standard practice in patients receiving pemetrexed. Reconstructed images were viewed using Osirix Imaging Software. Tumor SUV_{max} values were obtained by drawing volumes of interest over the tumor plane with the most active pixel and the two adjacent planes. In patients with multiple lesions, all evaluable (> 2 cm) lesions were assessed. The institutional review board at Wayne State University approved the study protocol. All patients signed a written informed consent.

Statistical Considerations

All statistical tests were conducted using GraphPad Prism version 6. For cellular tracer uptake studies, one-way analysis of variance was used. For animal studies, a paired sample analysis of variance adjusting for unequal sample size, when appropriate, was used.

RESULTS

Changes in ^3H -FLT Uptake Reflect Sensitivity to Dexamethasone

As discussed, the level of expression of GR α was found to be the deciding factor whether cells would be protected from pemetrexed following dexamethasone pretreatment. To determine whether dexamethasone sensitivity is associated with changes in FLT uptake, several NSCLC cell lines with varying expression of GR α were tested (Figs. 1A and 1B). In cells with the highest relative GR α expression there was a significant reduction in ^3H -FLT accumulation after 24h dexamethasone (Fig. 1C). ^3H -FLT retention was further decreased after 48 h, consistent with observed reduction of the S-phase fraction of cells ($P < 0.01$).

Dexamethasone Reversibly Decreases ^{18}F -FLT Retention in Human Xenografts

To evaluate whether ^{18}F -FLT-PET can detect dexamethasone sensitivity *in vivo*, mice implanted bilaterally with A549 tumors were imaged at baseline and after dexamethasone treatment. SUV_{max} in A549 tumors decreased by an average of 63.1% (Range: -70.5 to -54.70, SD: 5.08) following 24h dexamethasone (Fig. 2). 72 h post treatment, tumors regained their proliferative capacity and SUV_{max} values were in accordance with control tumors, indicating the reversibility of dexamethasone-mediated cell cycle arrest ($P < 0.01$).

To further establish the ability of ^{18}F -FLT to image the anti-proliferative effect of dexamethasone, mice bearing low-GR α H1299 tumors, as well as H1299 tumors in which GR α had been lentivirally transduced, were imaged. Similar to animals with A549 tumors, mice bearing H1299-GR α exhibited post-treatment reductions in tumor SUV_{max} (mean change: -41.3%, range: -53.0 to -11.6, SD: 14.9) that rebounded after 72 h dexamethasone withdrawal (Fig. 3). Interestingly, in H1299 tumors, which express low levels of GR α and were unaffected by dexamethasone in cell culture, a significant decrease in FLT accumulation was observed following dexamethasone treatment (mean change: -20.8%, range: -36.4 to 2.7, SD: 9.6) ($P < 0.01$). Harvested tumors revealed that although GR α mRNA levels remain lower in H1299 tumors than the other xenograft models used herein, populations of cells within H1299 tumors stained positive for GR (Supplemental Fig. 2). Critically, the

magnitude of reduction in tracer retention from baseline was associated with the relative GR α expression within the tumors.

¹⁸F-FLT Visualizes Interlesion Heterogeneity in Dexamethasone Sensitivity Between Metastases in Human Tumors

To determine whether these findings in NSCLC cell lines and xenografts were relevant to human disease, work was extended into four patients with advanced NSCLC. After dexamethasone treatment, tumors in patients #1 and #3 demonstrated marked reductions in tumor SUV_{max} from baseline (-64.7% and -54.3%, respectively). Conversely, patients #2 and #4 were largely unaffected by dexamethasone treatment, highlighting variability in the effect between patients (Table 1).

Furthermore, marked heterogeneity within individual patients was observed, as the lesions of patient #1 showed variable change in ¹⁸F-FLT uptake after dexamethasone (Fig. 4), whereas patient #3 showed the effect in all lesions. Unfortunately, these results could not be compared to tumor GR α expression due to insufficient tumor tissue available.

Dexamethasone Abolishes Pemetrexed-Mediated Flare in ³H-FLT Uptake in NSCLC Cell Lines

As mentioned, compounds that interfere with *de novo* thymidine biosynthesis, such as pemetrexed, can lead to a temporary upregulation in thymidine salvage, and therefore FLT accumulation, as cells seek to replenish intracellular thymidine exogenously. Exploiting this phenomenon may provide a method to monitor pemetrexed activity *in vivo*. To test this idea, ³H-FLT uptake was measured in NSCLC cells following 4h pemetrexed treatment (Fig. 5). ³H-FLT accumulation significantly increased in all cell lines (P < 0.01). However, 24h pretreatment with dexamethasone abrogated this effect in sensitive cell lines.

¹⁸F-FLT Visualizes Dexamethasone Interference with Pemetrexed Activity

To evaluate the flare effect *in vivo*, the xenograft models described in previous experiments were used. As was observed in cell culture, in mice implanted with A549 tumors ¹⁸F-FLT uptake increased by 48.9% from baseline (range: -3.5 to 102.5% SD: 33.9) after pemetrexed treatment, but this effect was abolished if animals received dexamethasone pretreatment (mean change: -44.5% from baseline, range: -65.8 to -22.7% SD: 15.56) (Fig. 6) P < 0.01. Following pemetrexed, H1299

tumors exhibited a greater flare from baseline than A549 xenografts: SUV_{max} in H1299 and H1299-GR α tumors increased by 107.3% (range: 11.6 to 268.5% SD: 90.4) and 68.7% (range: 0.0 to 164.5% SD: 57.4), respectively. If animals were pretreated with dexamethasone, the flare response was completely eradicated in H1299-GR α tumors, and the change from baseline resembled that of animals treated with dexamethasone alone (mean change: -42.9% from baseline, range: -67.4 to -18.9% SD: 15.56). H1299 tumors still exhibited a significant flare from baseline (mean change in SUV_{max} of 32.9%, range: -8.0 to 68.8% SD: 30.1), but it was smaller than that produced by pemetrexed alone, potentially reflecting GR upregulation (Fig. 7).

DISCUSSION

The treatment landscape for NSCLC is rapidly evolving with the introduction of newer targeted therapies and immune modulating agents. Despite these advances, the vast majority of patients diagnosed with advanced NSCLC will at some point receive platinum-based cytotoxic chemotherapy, often with pemetrexed. Here, the use of FLT retention was explored as a biomarker to monitor dexamethasone-mediated S-phase suppression in several models of NSCLC. Studies in NSCLC cell lines indicated that treatment with dexamethasone for 24h produced a significant reduction in ³H-FLT uptake in cell lines with relatively high GR α expression. This result was translatable to animal studies, where mice implanted with high-GR α A549 tumors demonstrated a significant reduction in tracer uptake after dexamethasone treatment. Furthermore, when imaging isogenic H1299 and H1299-GR α tumors, the magnitude of change in ¹⁸F-FLT retention in response to dexamethasone was associated to the expression level of GR α . Of note, low-GR H1299 tumors displayed an unexpected decline in ¹⁸F-FLT uptake following dexamethasone, a result that was discordant with in vitro studies. However, it is important to note that although H1299 cells express relatively low amounts of GR α , they are not GR α -negative. Further, GR has been shown to be involved in numerous cellular survival pathways and can be activated by conditions such as hypoxia, nutrient deprivation, and reactive oxygen species (31,32). Since cancer cell lines in ectopic xenografts face a more hostile growth medium than

those in cell culture, it is possible that stresses within the tumor microenvironment may preferentially support sub-populations of cells expressing higher levels of GR α , which could, in turn, lead to alterations in ^{18}F -FLT retention following glucocorticoids. Indeed, immunohistochemical staining of harvested tumors demonstrated clusters of GR-positive cells.

In patients with advanced NSCLC, the changes were much more variable, 2/4 patients showing some response to dexamethasone. Critically, ^{18}F -FLT PET was able to detect heterogeneity in dexamethasone sensitivity between lesions within individual patients. The capacity to simultaneously evaluate multiple lesions in patients is a major advantage of imaging compared to analysis of biopsy specimens, given that NSCLC patients receiving chemotherapy have advanced disease.

In addition, this study sought to use FLT accumulation to monitor pemetrexed activity through its inhibitory effect on TS, and subsequent increase in FLT accumulation. In agreement with recent studies, it was found that pemetrexed treatment produced a significant increase in ^3H -FLT retention compared to control (27). This effect was eradicated in high GR α -expressing cells if they were pretreated with dexamethasone. Animal imaging further corroborated this finding. Mice bearing A549 and H1299-GR α tumors exhibited a significant flare from baseline after pemetrexed treatment, which was prevented if animals received dexamethasone prior to chemotherapy. Conversely, low-GR α H1299 tumors produced a flare regardless of dexamethasone treatment. Taken together, these data suggest that the presence of a flare in response to pemetrexed may be indicative of the activity of the drug, and may be useful as an early marker for assessing response to therapy. A recent study in NSCLC patients treated with pemetrexed attempted to correlate a flare in ^{18}F -FLT uptake with drug efficacy. The study found only 2/11 subjects exhibited a flare, with the remaining individuals demonstrating either reduced or no change in tumor ^{18}F -FLT uptake after pemetrexed treatment. Furthermore, the flare did not correlate with response to therapy (33). However, all patients on study received dexamethasone prior to their treatment, this result may be due to dexamethasone-mediated

suppression of TK1, which counteracts the compensatory rise in thymidine salvage due to TS inhibition.

An unfortunate limitation of the present work was an inability to directly correlate changes in ^{18}F -FLT uptake after dexamethasone treatment with tumor GR α expression measured from patient biopsy samples due to insufficient available tumor tissue. Furthermore, no conclusions can be made regarding the impact of dexamethasone on the efficacy of pemetrexed chemotherapy in this particular cohort, as patients received other agents as part of their treatment regimen. Further work is needed to correlate tissue and image results regarding dexamethasone sensitivity and its impact on chemotherapy response. Despite its promise as an agent for monitoring S-phase suppression, ^{18}F -FLT has a number of noteworthy limitations. Cells that are highly reliant on *de novo* thymidine synthesis will have low baseline ^{18}F -FLT uptake, and therefore changes in tracer retention may be difficult to detect (34). In addition, tracer accumulation can be skewed at sites of inflammation, the presence of agents that alter the balance between the *de novo* and salvage pathways used for thymidine synthesis, or increased cellular clearance of FLT-phosphate (k₄) (35-37).

CONCLUSION

Ultimately, the imaging approach used here could allow for the stratification of patient tumors by dexamethasone sensitivity. Patients found to have one or more dexamethasone-sensitive lesions could be given a treatment regimen that does not require dexamethasone prophylaxis. Alternatively, it may facilitate adjustment of the dexamethasone treatment schedule such that the interference with therapy could be minimized while still preventing adverse events. More generally, numerous studies have found that glucocorticoids, through various mechanisms, reduce the efficacy of commonly used anti-neoplastic agents including cisplatin, doxorubicin, and gemcitabine (38-40). This effect has been shown in models of breast, brain, colon, prostate, and cervical cancer, among others (41). ^{18}F -FLT-PET is a potential tool to detect this phenomenon, which may critically impact patient outcomes, as many chemotherapeutic agents are given with glucocorticoids as part of supportive care.

ACKNOWLEDGEMENTS The authors wish to acknowledge Dr. Larry Matherly for his helpful guidance regarding the use of antifolates in rodents and Dr. Mugdha Patki for her assistance optimizing cellular studies.

REFERENCES

1. Siegel RL, Miller KD, Jemal A. Cancer Statistics, 2017. *CA Cancer J Clin.* 2017;67:7-30.
2. Hanna N, Shepherd FA, Fossella FV, et al. Randomized phase III trial of pemetrexed versus docetaxel in patients with non-small-cell lung cancer previously treated with chemotherapy. *J Clin Oncol.* 2004;22:1589-1597.
3. Patel JD, Socinski MA, Garon EB, et al. PointBreak: a randomized phase III study of pemetrexed plus carboplatin and bevacizumab followed by maintenance pemetrexed and bevacizumab versus paclitaxel plus carboplatin and bevacizumab followed by maintenance bevacizumab in patients with stage IIIB or IV nonsquamous non-small-cell lung cancer. *J Clin Oncol.* 2013;31:4349-4357.
4. Scagliotti GV, Parikh P, von Pawel J, et al. Phase III study comparing cisplatin plus gemcitabine with cisplatin plus pemetrexed in chemotherapy-naive patients with advanced-stage non-small-cell lung cancer. *J Clin Oncol.* 2008;26:3543-3551.
5. Chattopadhyay S, Moran RG, Goldman ID. Pemetrexed: biochemical and cellular pharmacology, mechanisms, and clinical applications. *Mol Cancer Ther.* 2007;6:404-417.
6. Shih C, Habeck LL, Mendelsohn LG, Chen VJ, Schultz RM. Multiple folate enzyme inhibition: mechanism of a novel pyrrolopyrimidine-based antifolate LY231514 (MTA). *Adv Enzyme Regul.* 1998;38:135-152.
7. Gridelli C, Kaukel E, Gregorc V, et al. Single-agent pemetrexed or sequential pemetrexed/gemcitabine as front-line treatment of advanced non-small cell lung cancer in elderly patients or patients ineligible for platinum-based chemotherapy: a multicenter, randomized, phase II trial. *J Thorac Oncol.* 2007;2:221-229.
8. Cetin K, Ettinger DS, Hei YJ, O'Malley CD. Survival by histologic subtype in stage IV nonsmall cell lung cancer based on data from the Surveillance, Epidemiology and End Results Program. *Clin Epidemiol.* 2011;3:139-148.

9. Liu Y, Yin TJ, Zhou R, Zhou S, Fan L, Zhang RG. Expression of thymidylate synthase predicts clinical outcomes of pemetrexed-containing chemotherapy for non-small-cell lung cancer: a systemic review and meta-analysis. *Cancer Chemother Pharmacol*. 2013;72:1125-1132.
10. Wynes MW, Konopa K, Singh S, et al. Thymidylate synthase protein expression by IHC and gene copy number by SISH correlate and show great variability in non-small cell lung cancer. *J Thorac Oncol*. 2012;7:982-992.
11. Rusthoven JJ, Eisenhauer E, Butts C, et al. Multitargeted antifolate LY231514 as first-line chemotherapy for patients with advanced non-small-cell lung cancer: A phase II study. National Cancer Institute of Canada Clinical Trials Group. *J Clin Oncol*. 1999;17:1194.
12. Scagliotti G, Hanna N, Fossella F, et al. The differential efficacy of pemetrexed according to NSCLC histology: a review of two Phase III studies. *Oncologist*. 2009;14:253-263.
13. Basch E, Prestrud AA, Hesketh PJ, et al. Antiemetics: American Society of Clinical Oncology clinical practice guideline update. *J Clin Oncol*. 2011;29:4189-4198.
14. Vilasco M, Communal L, Mourra N, Courtin A, Forgez P, Gompel A. Glucocorticoid receptor and breast cancer. *Breast Cancer Res Treat*. 2011;130:1-10.
15. Schaaf MJ, Cidlowski JA. Molecular mechanisms of glucocorticoid action and resistance. *J Steroid Biochem Mol Biol*. 2002;83:37-48.
16. Patki M, Gadgeel S, Huang Y, et al. Glucocorticoid receptor status is a principal determinant of variability in the sensitivity of non-small-cell lung cancer cells to pemetrexed. *J Thorac Oncol*. 2014;9:519-526.
17. Lu YS, Lien HC, Yeh PY, et al. Glucocorticoid receptor expression in advanced non-small cell lung cancer: clinicopathological correlation and in vitro effect of glucocorticoid on cell growth and chemosensitivity. *Lung Cancer*. 2006;53:303-310.
18. Gerlinger M, Rowan AJ, Horswell S, et al. Intratumor heterogeneity and branched evolution revealed by multiregion sequencing. *N Engl J Med*. 2012;366:883-892.

19. Fidler IJ. Tumor heterogeneity and the biology of cancer invasion and metastasis. *Cancer Res.* 1978;38:2651-2660.
20. Tehrani OS, Douglas KA, Lawhorn-Crews JM, Shields AF. Tracking cellular stress with labeled FMAU reflects changes in mitochondrial TK2. *Eur J Nucl Med Mol Imaging.* 2008;35:1480-1488.
21. Shields AF, Grierson JR, Dohmen BM, et al. Imaging proliferation in vivo with [F-18]FLT and positron emission tomography. *Nat Med.* 1998;4:1334-1336.
22. Chalkidou A, Landau DB, Odell EW, Cornelius VR, O'Doherty MJ, Marsden PK. Correlation between Ki-67 immunohistochemistry and 18F-fluorothymidine uptake in patients with cancer: A systematic review and meta-analysis. *Eur J Cancer.* 2012;48:3499-3513.
23. Shields AF, Lawhorn-Crews JM, Briston DA, et al. Analysis and reproducibility of 3'-Deoxy-3'-[18F]fluorothymidine positron emission tomography imaging in patients with non-small cell lung cancer. *Clin Cancer Res.* 2008;14:4463-4468.
24. Tehrani OS, Shields AF. PET imaging of proliferation with pyrimidines. *J Nucl Med.* 2013;54:903-912.
25. Dittmann H, Dohmen BM, Kehlbach R, et al. Early changes in [18F]FLT uptake after chemotherapy: an experimental study. *Eur J Nucl Med Mol Imaging.* 2002;29:1462-1469.
26. Saito Y, Furukawa T, Arano Y, Fujibayashi Y, Saga T. Comparison of semiquantitative fluorescence imaging and PET tracer uptake in mesothelioma models as a monitoring system for growth and therapeutic effects. *Nucl Med Biol.* 2008;35:851-860.
27. Chen X, Yang Y, Katz S. Early detection of thymidylate synthase resistance in non-small cell lung cancer with FLT-PET imaging. *Oncotarget.* 2017;8:82705-82713.
28. Dandona P, Mohanty P, Hamouda W, Aljada A, Kumbkarni Y, Garg R. Effect of dexamethasone on reactive oxygen species generation by leukocytes and plasma interleukin-10 concentrations: a pharmacodynamic study. *Clin Pharmacol Ther.* 1999;66:58-65.

- 29.** Bhadri VA, Cowley MJ, Kaplan W, Trahair TN, Lock RB. Evaluation of the NOD/SCID xenograft model for glucocorticoid-regulated gene expression in childhood B-cell precursor acute lymphoblastic leukemia. *BMC Genomics*. 2011;12:565.
- 30.** Shields AF, Grierson JR, Muzik O, et al. Kinetics of 3'-deoxy-3'-[F-18]fluorothymidine uptake and retention in dogs. *Mol Imaging Biol*. 2002;4:83-89.
- 31.** Leonard MO, Godson C, Brady HR, Taylor CT. Potentiation of glucocorticoid activity in hypoxia through induction of the glucocorticoid receptor. *J Immunol*. 2005;174:2250-2257.
- 32.** Regan Anderson TM, Ma SH, Raj GV, et al. Breast Tumor Kinase (Brk/PTK6) Is Induced by HIF, Glucocorticoid Receptor, and PELP1-Mediated Stress Signaling in Triple-Negative Breast Cancer. *Cancer Res*. 2016;76:1653-1663.
- 33.** Frings V, van der Veldt AA, Boellaard R, et al. Pemetrexed induced thymidylate synthase inhibition in non-small cell lung cancer patients: a pilot study with 3'-deoxy-3'-[(1)(8)F]fluorothymidine positron emission tomography. *PLoS One*. 2013;8:e63705.
- 34.** McKinley ET, Ayers GD, Smith RA, et al. Limits of [18F]-FLT PET as a biomarker of proliferation in oncology. *PLoS One*. 2013;8:e58938.
- 35.** Lee SJ, Kim SY, Chung JH, et al. Induction of thymidine kinase 1 after 5-fluorouracil as a mechanism for 3'-deoxy-3'-[18F]fluorothymidine flare. *Biochem Pharmacol*. 2010;80:1528-1536.
- 36.** Troost EG, Vogel WV, Merks MA, et al. 18F-FLT PET does not discriminate between reactive and metastatic lymph nodes in primary head and neck cancer patients. *J Nucl Med*. 2007;48:726-735.
- 37.** Muzi M, Vesselle H, Grierson JR, et al. Kinetic analysis of 3'-deoxy-3'-fluorothymidine PET studies: validation studies in patients with lung cancer. *J Nucl Med*. 2005;46:274-282.
- 38.** Morita M, Suyama H, Igishi T, et al. Dexamethasone inhibits paclitaxel-induced cytotoxic activity through retinoblastoma protein dephosphorylation in non-small cell lung cancer cells. *Int J Oncol*. 2007;30:187-192.
- 39.** Gassler N, Zhang C, Wenger T, et al. Dexamethasone-induced cisplatin and gemcitabine resistance in lung carcinoma samples treated ex vivo. *Br J Cancer*. 2005;92:1084-1088.

40. Braunschweiger PG, Ting HL, Schiffer LM. Receptor-mediated antiproliferative effects of corticosteroids in Lewis lung tumors. *Eur J Cancer Clin Oncol.* 1984;20:427-433.
41. Mattern J, Buchler MW, Herr I. Cell cycle arrest by glucocorticoids may protect normal tissue and solid tumors from cancer therapy. *Cancer Biol Ther.* 2007;6:1345-1354.

FIGURES

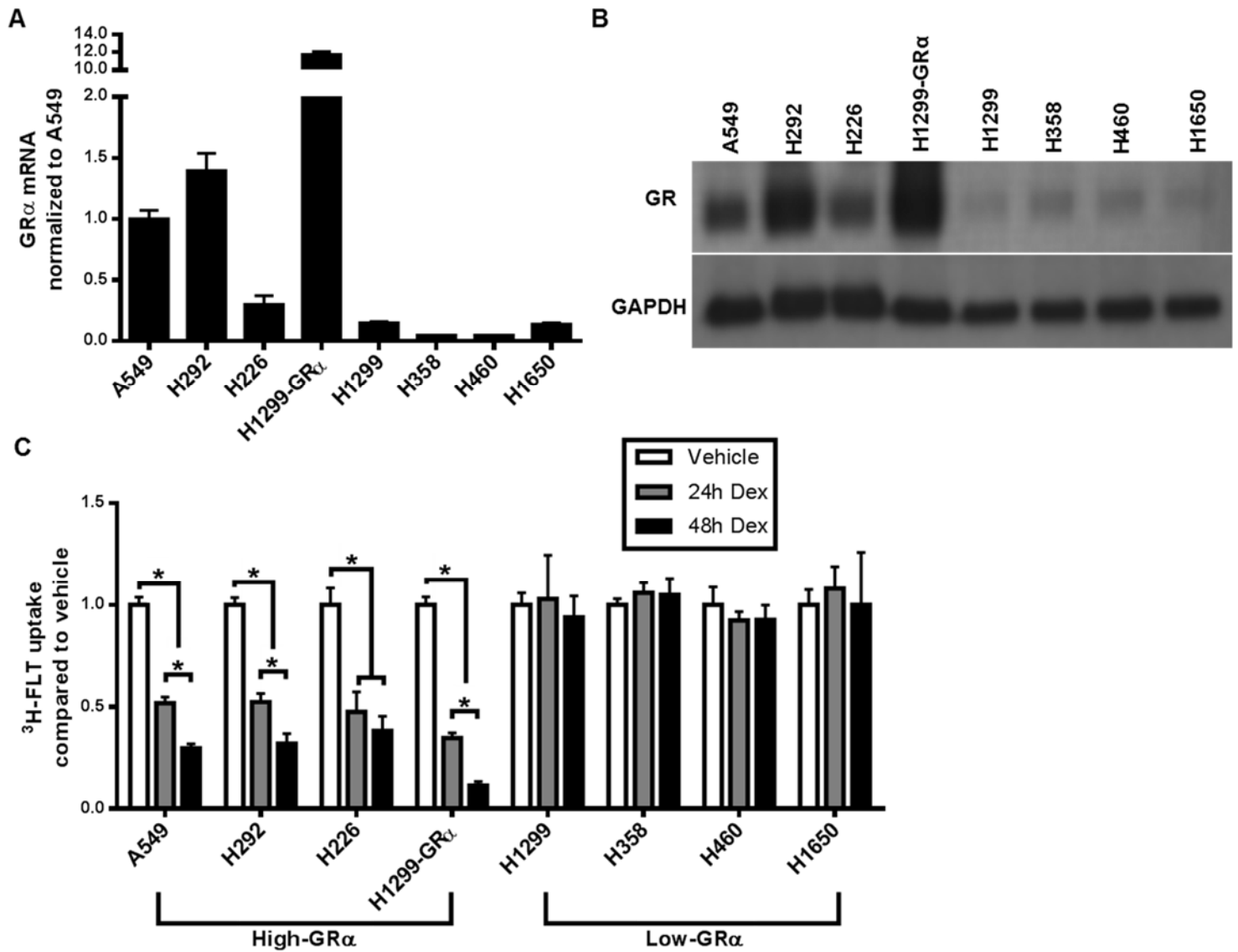


FIGURE 1: Effect of Dexamethasone on FLT Retention in NSCLC Cell Lines with Varying GR α Expression. A) GR α mRNA measured by RT-PCR. B) Western blot showing total GR protein expression. C) ³H-FLT in NSCLC cell lines after 24h and 48h dexamethasone (Dex). *P < 0.01.

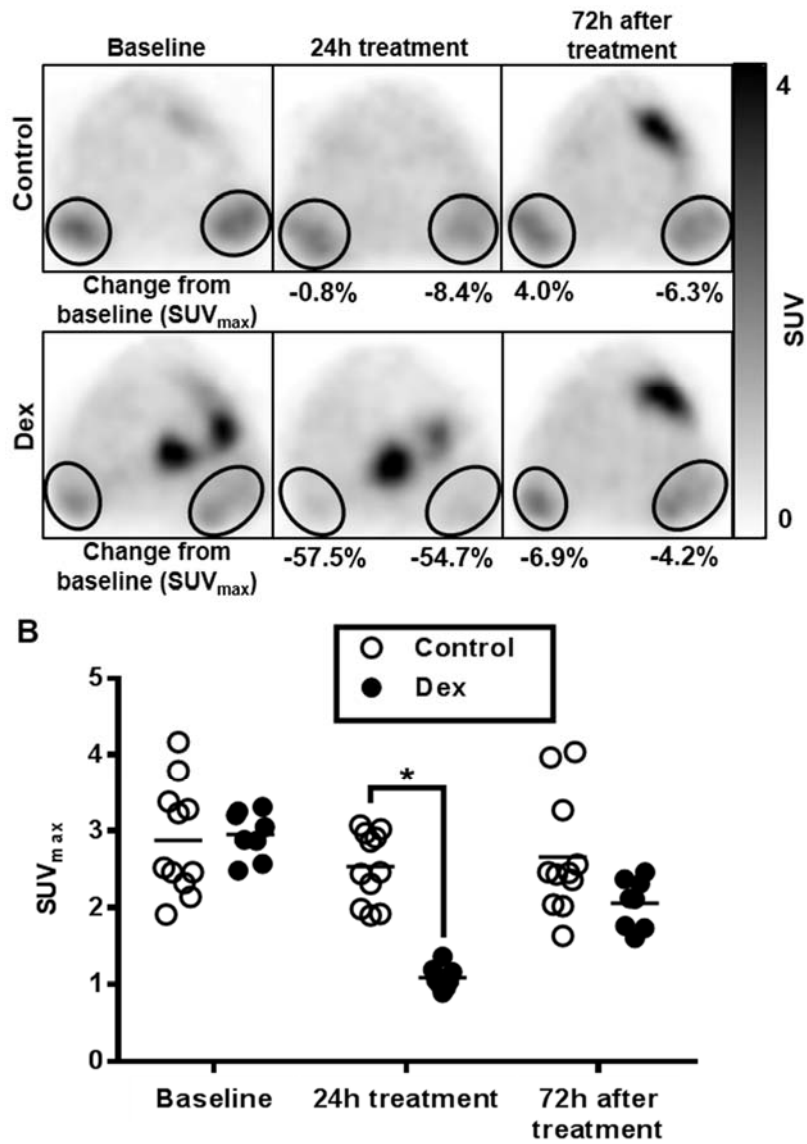


FIGURE 2: Dexamethasone Reduces ¹⁸F-FLT Accumulation in Mice Bearing A549 Tumors. A) Representative images of animals treated with dexamethasone or control (saline). B) Dot plot expressing tumor SUV_{max} values of tumors treated with dexamethasone (Dex) or control. *P < 0.01

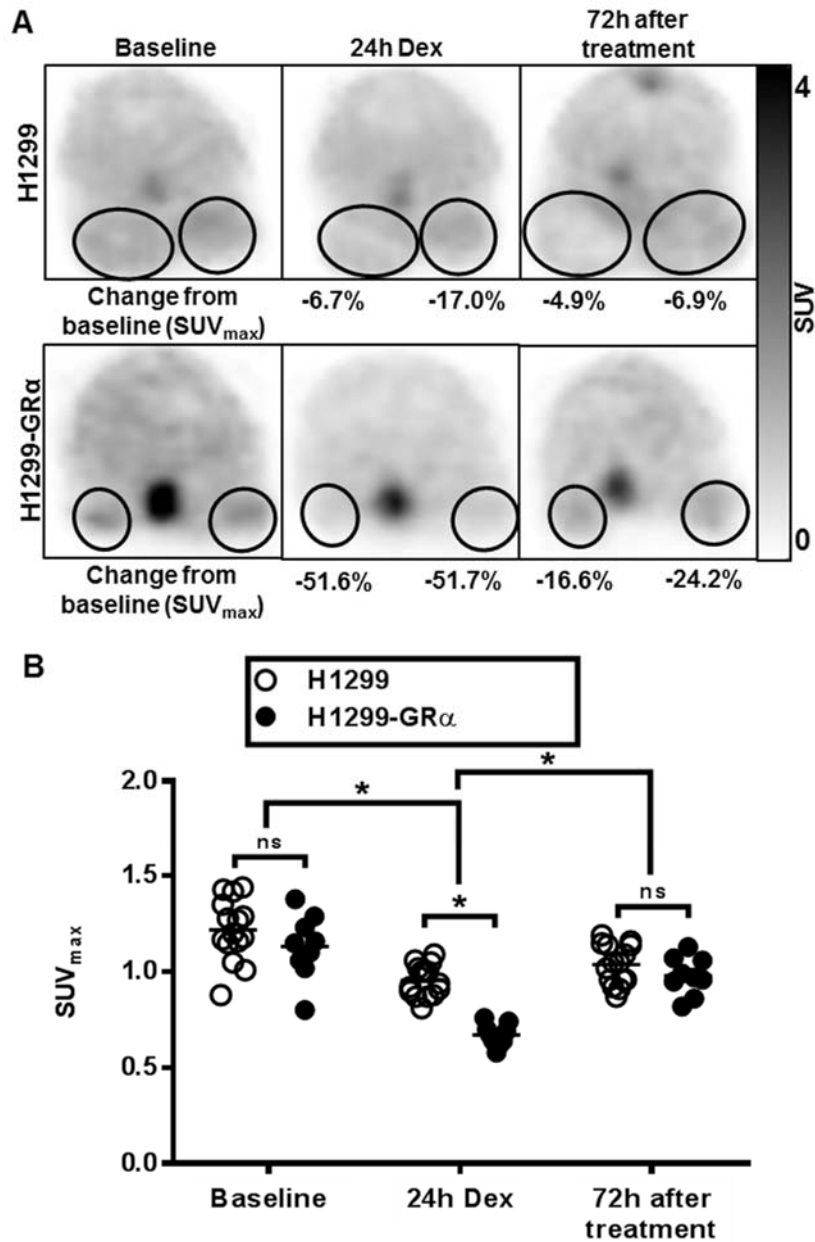


FIGURE 3: Decline in ^{18}F -FLT Retention Following Dexamethasone depends on GR α

Expression. A) Representative images of animals implanted with H1299 or H1299-GR α tumors (circles) before and after dexamethasone (Dex). B) Dot-plot comparing SUV_{max} values of H1299 tumors with H1299-GR α . *P < 0.01.

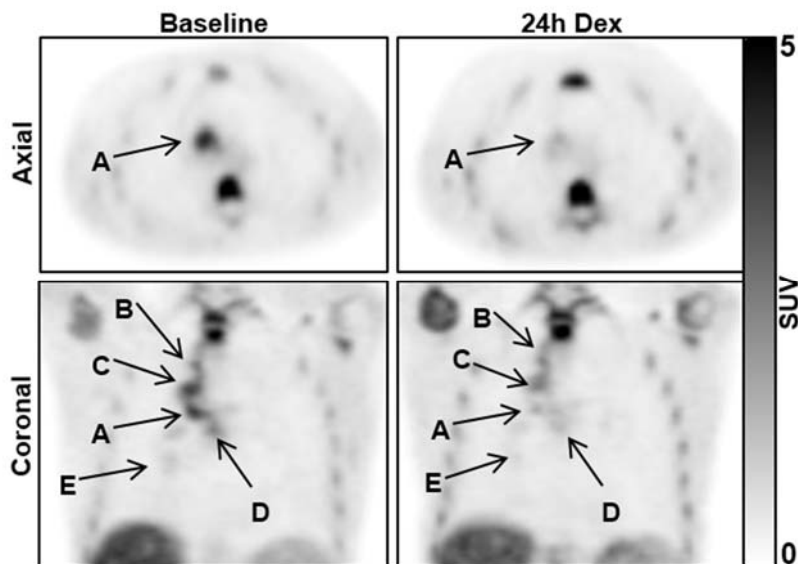


FIGURE 4: ^{18}F -FLT-PET Captures Interlesion Heterogeneity.

^{18}F -FLT-PET images from a patient with NSCLC at baseline (left) and after 24h dexamethasone. In the nodal metastasis indicated 'A', ^{18}F -FLT uptake decreased by 64.7% after 24h dexamethasone. Tracer retention in lesions indicated by 'B', 'C', 'D', and 'E' decreased by 13.7%, 33.1%, 18.1%, and 34.6% respectively. Vertebral, sternal, and rib marrow activity was unchanged.

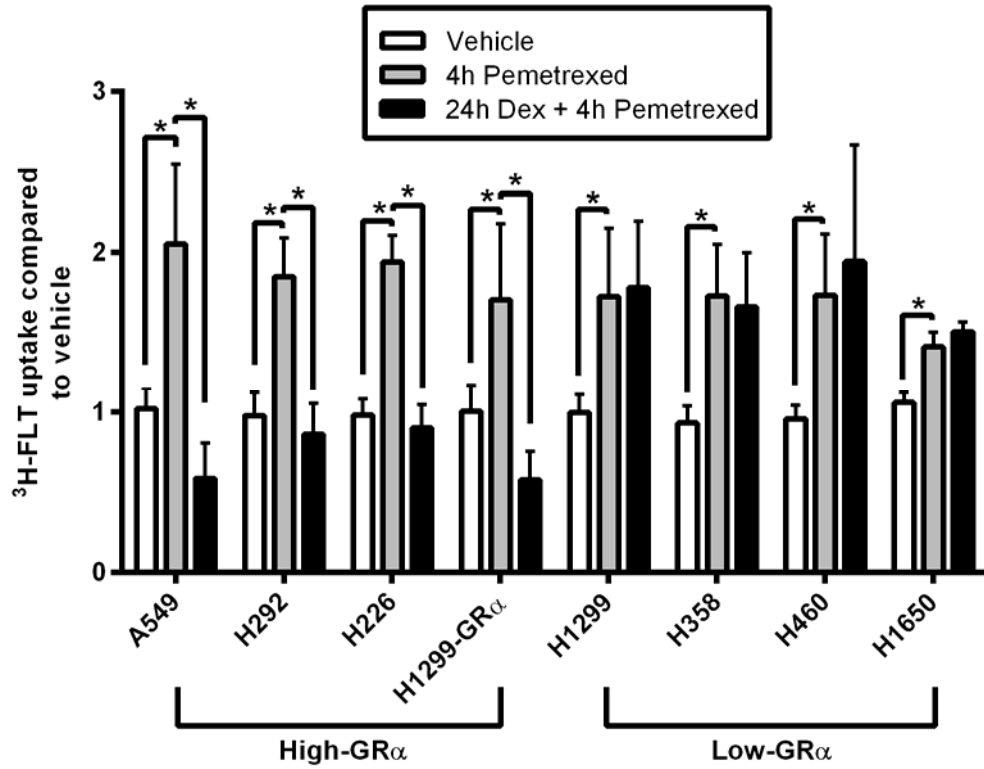


FIGURE 5: Effect of Dexamethasone and Pemetrexed on FLT Retention in NSCLC Cell Lines.

$^3\text{H-FLT}$ uptake in NSCLC cells were treated with pemetrexed or vehicle (saline) with or without pretreatment with dexamethasone (Dex) for 24h. *P < 0.01

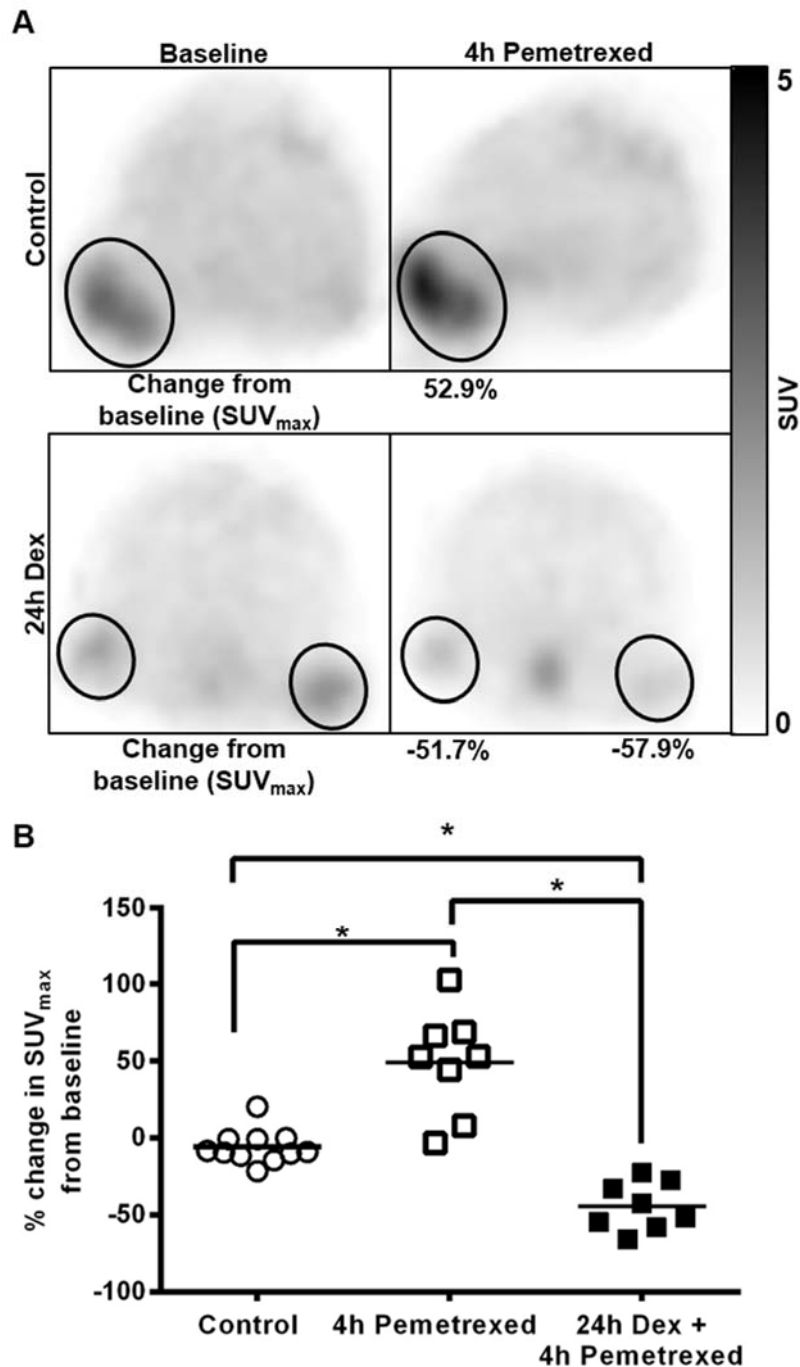


FIGURE 6: Pemetrexed-Induced Flare in ¹⁸F-FLT Uptake is Abolished with Dexamethasone Pretreatment in Animal Xenografts. A) Representative images of a mouse bearing A549 tumors are shown (circles). B) Dot plot depicting the change in SUV_{max} from baseline in mice treated with control (saline), 4h pemetrexed, and 4h pemetrexed with dexamethasone (Dex) pretreatment *P < 0.01.

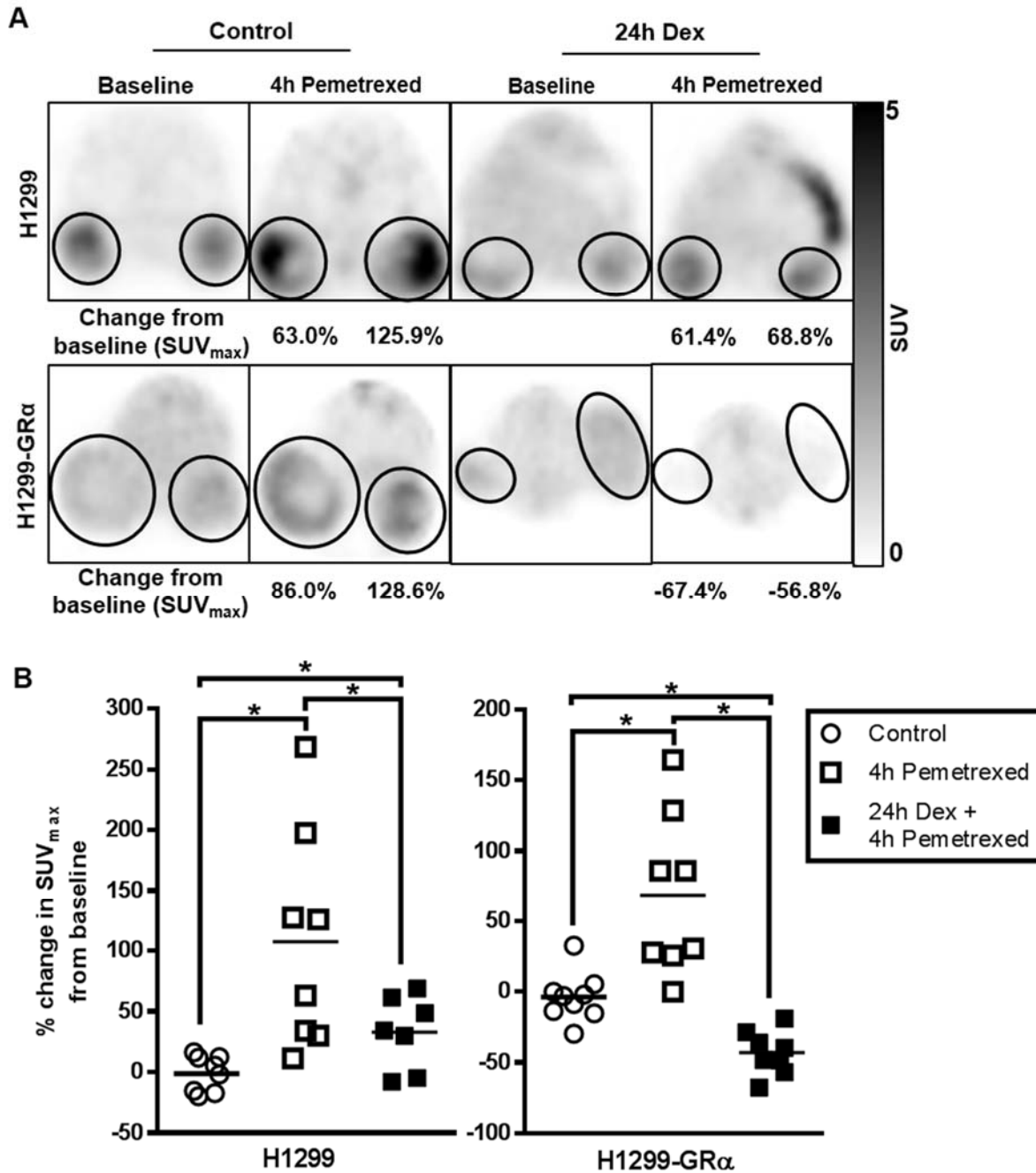
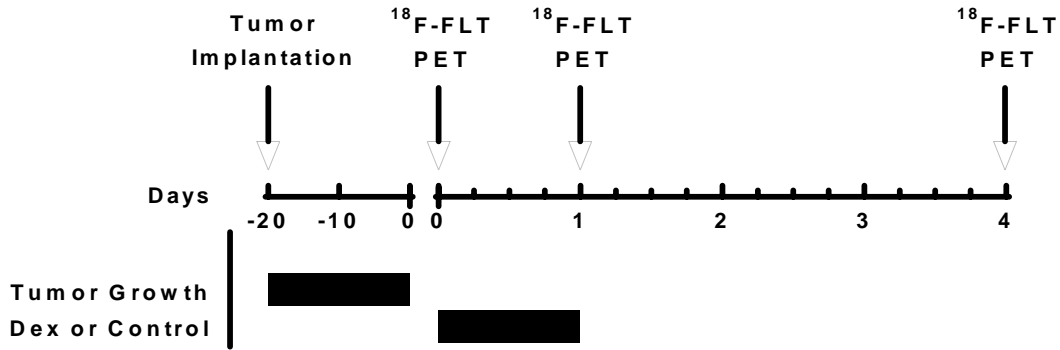


FIGURE 7: Eradication of Pemetrexed-Induced Flare by Dexamethasone Occurs in a GR α -Dependent Fashion. A) Representative images from one animal with each condition are displayed. B) Dot plot displaying the effect of pemetrexed on ^{18}F -FLT retention in H1299 and H1299-GR α tumors, with or without dexamethasone (Dex) pretreatment. *P < 0.01.

Patient	Lesion	Baseline (SUV_{max})	24h Dexamethasone (SUV_{max})	% Change from Baseline
1	Primary Lesion	3.60	2.07	-42.6
	Lymph Node A	4.02	1.42	-64.7
	Lymph Node B	3.89	3.36	-13.7
	Lymph Node C	3.79	2.54	-33.1
	Lymph Node D	3.32	2.72	-18.1
	Lymph Node E	2.34	1.53	-34.4
2	Primary Lesion	8.42	7.22	-14.3
	Lymph Node A	5.74	4.60	-19.9
	Lymph Node B	5.18	5.04	-2.80
3	Primary Lesion	3.26	2.07	-36.4
	Lymph Node A	2.36	1.77	-25.1
	Lymph Node B	1.64	0.75	-54.3
	Lymph Node C	1.49	0.85	-42.8
4	Tumor A	2.08	1.85	-11.4
	Tumor B	4.00	3.43	-14.3
	Lymph Node A	6.13	6.83	11.5
	Lymph Node B	4.90	4.07	-17.0
	Lymph Node C	3.48	1.93	-44.6

Table 1: Change in Tumor ¹⁸F-FLT Uptake in NSCLC Patients After Dexamethasone.

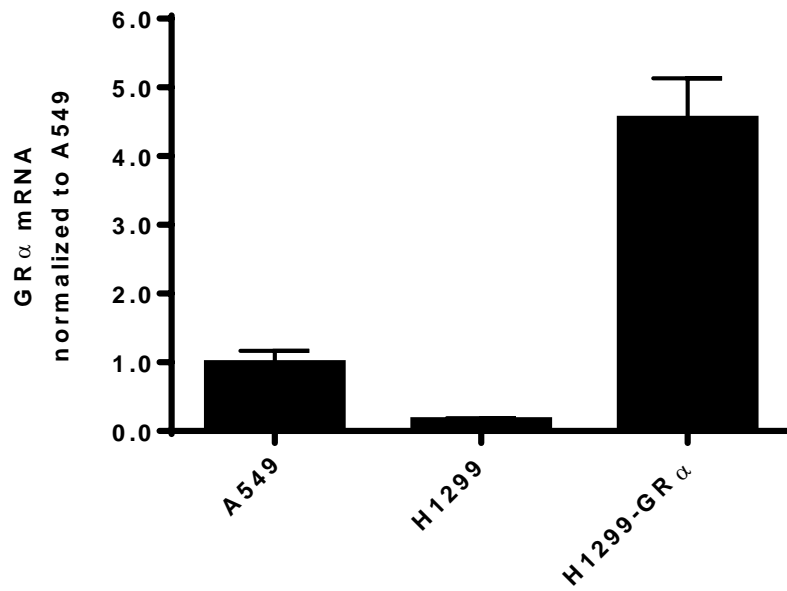
Supplementary Materials



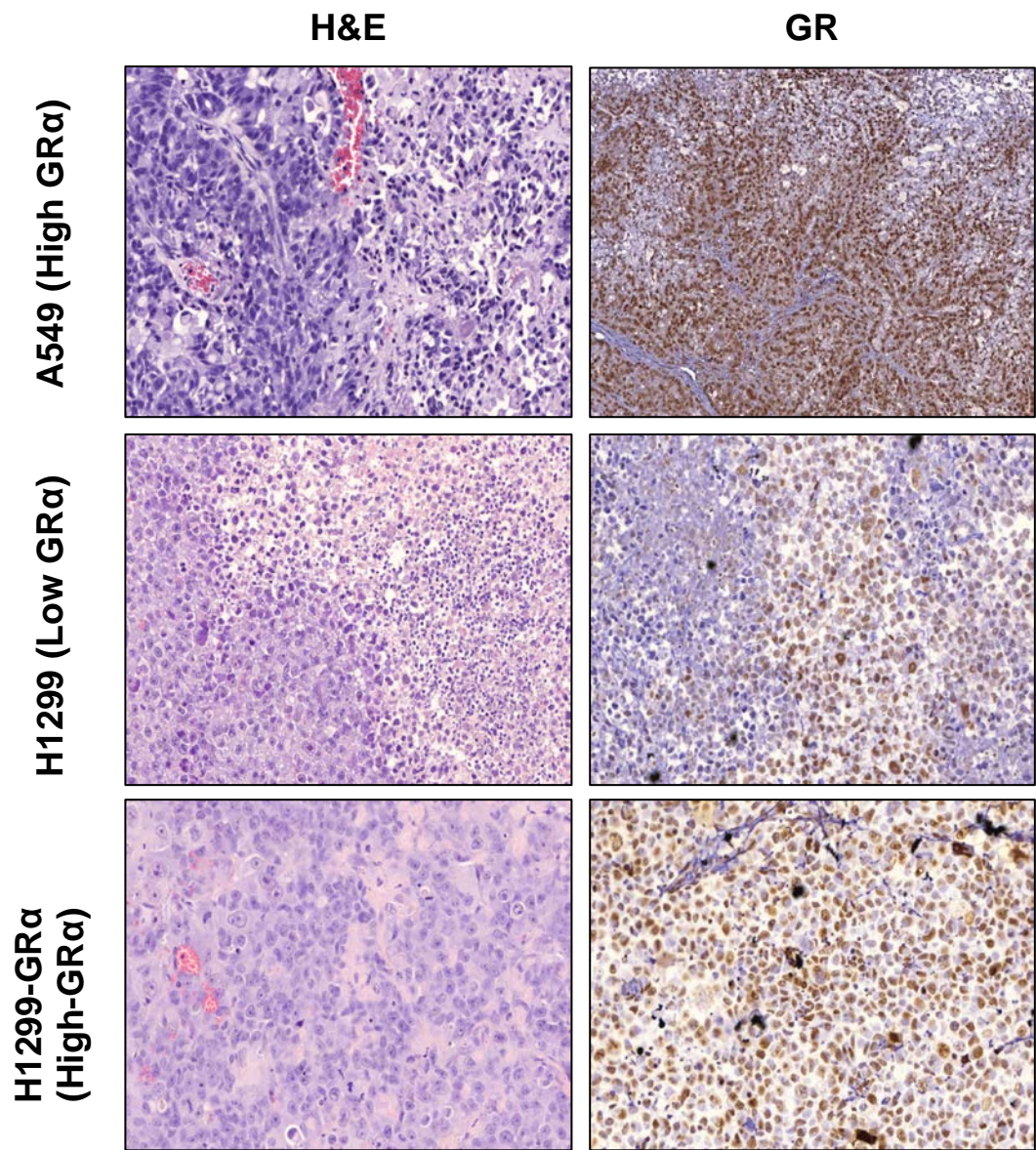
Supplemental Figure. 1: Dexamethasone Treatment and Animal Imaging Protocol. 4-6 week-old female SCID/NCr mice were implanted with A549 or H1299 xenografts via trocar. After a 10-25 day period of tumor growth animals were imaged at baseline (Scan 1), after 24 h of treatment with dexamethasone (Dex) or control, and again 72 h after the final treatment to assess reversibility.

Sampling Time (h)	Serum Dex Concentration (nM)
Pre-dose	22
Pre-dose	28
2	4970
2	8140
12	61
12	14
24	0
24	0

Supplemental Table 1: Serum Dexamethasone Concentration. To ensure that animals were exposed to a pharmacologically relevant dose of dexamethasone between scans, mice were treated with 3 doses of dexamethasone (15 mg/kg ip, every 12 h). Blood samples were collected at four time points: prior to the third the final dose (pre-dose), 2, 12, and 24 h later. Serum samples were collected from two mice at each time point. Serum dexamethasone concentration was determined by liquid chromatography-mass spectrometry.



Supplemental Fig. 2A: GR α mRNA in human xenografts. Tumors were harvested and GR α mRNA was measured by RT-PCR. Error bars represent standard deviation between biological triplicate samples.



Supplemental Fig. 2B: GR staining in human xenografts. Representative pictures of tumors stained with hematoxylin and eosin (left) or an anti-GR antibody.